A. Suresh Kumar, S. Nagaraja Rao, P.Balaji / International Journal of Engineering Research and Applications (IJERA) ISSN: 2248-9622 www.ijera.com
Vol. 2, Issue 4, July-August 2012, pp.889-895

An Improved ZVZCS Full Bridge Converter with secondary Resonance for High Power Applications

***A. Suresh Kumar **S. Nagaraja Rao ***P.Balaji**
*Assistant Professor, Dept. of EEE, RGMCET, Nandyal
**Assistant Professor, Dept. of EEE, RGMCET, Nandyal
*******P.G.Student Dept. of EEE, RGMCET,

ABSTRACT-

A new zero voltage and zero currentswitching (ZVZCS) full bridge (FB) PWM converter is proposed to improve the performance of the previously presented ZVZCS-FB-PWM converters. In the proposed circuit leakage inductance of the transformer is utilized as secondary resonance with out an additional inductance. The ZVZCS means mixed operation of zero-voltage switching (ZVS) for leading-leg switches and zero-current switching (ZCS) for lagging-leg switches. The primary side of the converter is composed of FB insulated-gate bipolar transistors, which are driven by phase-shift control. The secondary side is composed of a resonant tank and a half-wave rectifier. Without an auxiliary circuit, zero-voltage switching (for leading-leg switches) and zero-current switching (for lagging-leg switches) are achieved in the entire operating range. These days, IGBTs are replacing MOSFETs for high voltage, high power applications, since IGBTs have higher voltage rating, higher power density, and lower cost compared to MOSFETs. The analysis and design considerations of the proposed converter are presented.

I. INTRODUCTION

IN high-frequency and high-power converters, it is desirable to use insulated-gate bipolar transistors (IGBTs) for primary switches and to utilize soft-switching techniques such as zero voltage switching (ZVS) and zero-current switching (ZCS)[1]-[24]. IGBTs can handle higher voltage and higher power with lower cost compared with MOSFETs, so IGBTs have been Replacing MOSFETs in applications requiring several or several tens of kilowatt power. In high-frequency converters, soft-switching techniques are widely used to reduce the switching loss that results from high switching frequency.

Among previous soft-switching FB converters, a series-resonant converter (SRC) [14]–[21] is the simplest topology. Moreover, because all switches of the converter are turned on at zero voltage, the conversion efficiency is relatively high. However, the SRC has some drawbacks. First, the output voltage cannot be regulated for the no-load case. Second, it has some difficulties, such as size reduction and a design of an electromagnetic-interference noise filter because a wide variation of the switching frequency is necessary to control the output voltage.

Some modified converters based on a conventional SRC have been presented to solve these problems. One is a converter that utilizes other control methods without additional hardware [22]–[24]. By using a control method in [22], regulation problems under low-power conditions can be solved, but the range of the operating frequency is still wide. Another presented approach is the phase-shift control of SRC, such as the ZVS FB converters in [23] and [24]. The ZVS FB converters can achieve constant-frequency operation, no regulation problem, and ZVS of all switches that are composed of MOSFETs. Because all switches of the converters are MOSFETs, the converters are not adequate for high-power conversion in the power range of several or tens of kilowatts. To apply the converter for high-power conversions, further improvements, such as applying IGBTs and extending the soft-switching range, are necessary.

The proposed converter has several advantages over existing converters. First, the leading-leg switches can be turned on softly under almost all operating conditions, and a lossless turn-off snubber can be used to reduce turn-off loss. Second, the lagging-leg switches can be turned on at zero voltage and also turned off near zero current without additional auxiliary circuits. Third, the reverse-recovery currents of the diodes are significantly reduced, and the voltage stresses of the output diodes are clamped to the output voltage. Therefore, last, the switching loss of the converter is very low, and the converter is adequate for high-voltage and high-power applications.

II. PRINCIPAL OF OPERATION

The operation of the converter in Fig. 1 is analyzed in this section. The output voltage *Vo* of the converter is controlled as in a conventional phase-shifted FB converter. The converter has six operation modes within each switching period *Ts*.

The operation waveforms and equivalent circuits are shown in Figs. 2 and 3, respectively. To analyze the operation of the converter, several assumptions are made in the following.

1) Leading-leg switches *T*1 and *B*1 and lagging-leg switches *T*2 and *B*2 are ideal, except for their body diodes.

2) Because the output capacitor *Co* is very large, the output voltage *Vo* is a dc voltage without any ripple.

3) Transformer *T* is composed of ideal transformers *N*1 and *N*2, a magnetizing inductance *Lm*, and a leakage inductance *L*lk.

4) Since the capacitances of lossless turn-off snubber (*CT*1 and *CB*1) are very small, the transient time of charging and discharging is neglected.

5) When the switching frequency *fs* is less than the resonant frequency *fr*, the conduction loss is large unnecessarily due to the high peak currents of the devices. Therefore, we assume that $fs \geq fr$.

The voltage across *N*2 is given as three-level voltages: *n*V*in*, 0, and −*n*V*in* by the phase-shift control of the primary switches, where *n* is the transformer turn ratio *N*2/*N*1 and *V*in is the input voltage. The series-resonant tank is formed by *L*lk and a resonant capacitor *Cr*, the secondary current *is* through the resonant circuit is half-wave rectified by the rectifying diodes *D*1 and *D*2, and the positive value of *is* feeds the output stage.

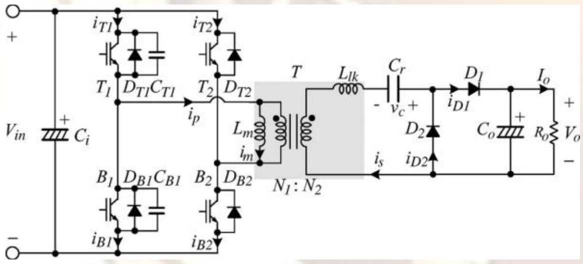

Fig. 1. *Proposed soft-switching FB converter with secondary resonance.*

A detailed mode analysis is as follows.

Mode 1 [*t*0, *t*1]*:* As shown in Figs. 2 and 3, top switches *T*1 and *T*2 are ON state, and *is* becomes zero at *t*0. During this mode, diodes *D*1 and *D*2 are OFF state, and the current *is* remains zero. Because the voltages across both *N*1 and *N*2 are zero, the magnetizing current *im* is constant. The following equalities are satisfied.

$$i_m(t) = i_p(t) = i_{T1}(t) = -i_{T2}(t) = i_m(t_2) \qquad (1)$$

Where *ip* is the primary current and *iT*1 is the sum of the currents of *T*1, its body diodes DT1's, and its snubber capacitance*CT*1. Similarly, *iT*2, *iB*1, and *iB*2 are defined. the currents of body diodes are simply the negative portions of *iT*1, *iT*2, *iB*1, and *iB*2.

Mode 2 [*t*1, *t*2]*:* At *t*1, the lagging-leg switch *T*2 is turned off when *iT*2 = −*im*. Because *im* is a very low current, *T*2 is turned off near zero current. After a short dead time, *B*2 is turned on at zero voltage, while the current *ip* flows through the body diode of *B*2. During this mode, the secondary voltage across *N*2 is *nV*in. Therefore, *is* builds up from its zero value and flows through *D*1. The state equations can be written as follows:

$$L_{lk}\frac{di_s(t)}{dt} + V_0 - v_c(t) = nV_{in}$$
$$C_r\frac{d(V_0 - v_c(t))}{dt} = i_s(t)$$
$$i_s(t) = 0 \qquad (2)$$

where *vc* is a voltage across *Cr*. Thus, *is* is obtained as

$$i_s(t) = \frac{nV_{in} - (V_0 - v_c(t_1))}{Z_0}\sin\omega_r(t - t_1) \qquad (3)$$

where the angular resonance frequency

$$\omega_r = 2\Pi f_r = \frac{1}{\sqrt{L_{lk}C_r}} \qquad (4)$$

and the characteristic impedance

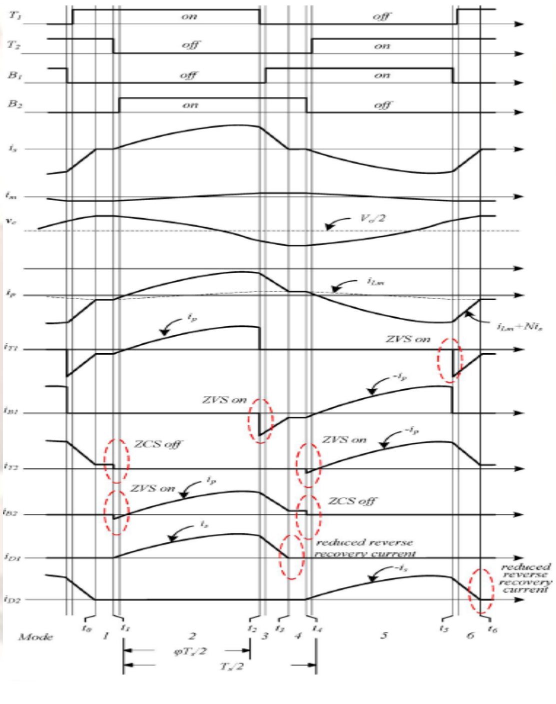

Fig:2 *:operational waveforms of proposed converter*

$$Z_0 = \sqrt{\frac{L_r}{C_r}} \qquad (5)$$

The magnetizing current *im* is increased linearly by the input voltage as

$$i_m(t)=i_m(t_1)+\frac{V_{in}}{L_m}(t-t_1) \quad (6)$$

The following equalities are also satisfied:

$$i_p(t)=i_m(t)=ni_s(t)=i_{T1}(t)=i_{B2}(t) \quad (7)$$

Mode 3 [*t*2, *t*3]*:* At *t*2, *T*1 is turned off .Subsequently, the current *ip* charges *CT*1 and discharges *CB*1. Once the collector–emitter voltage of *B*1 reaches zero, the current *ip* flows through the body diode of *B*1. After dead time, *B*1 is turned on at zero voltage. Because the voltage across *N*2 is zero, *is* goes to zero. The state equation is the same as (2), except for the initial condition of *is* and the applied voltage across *N*2.Thus, the current *is* can be obtained analogously with (3) as

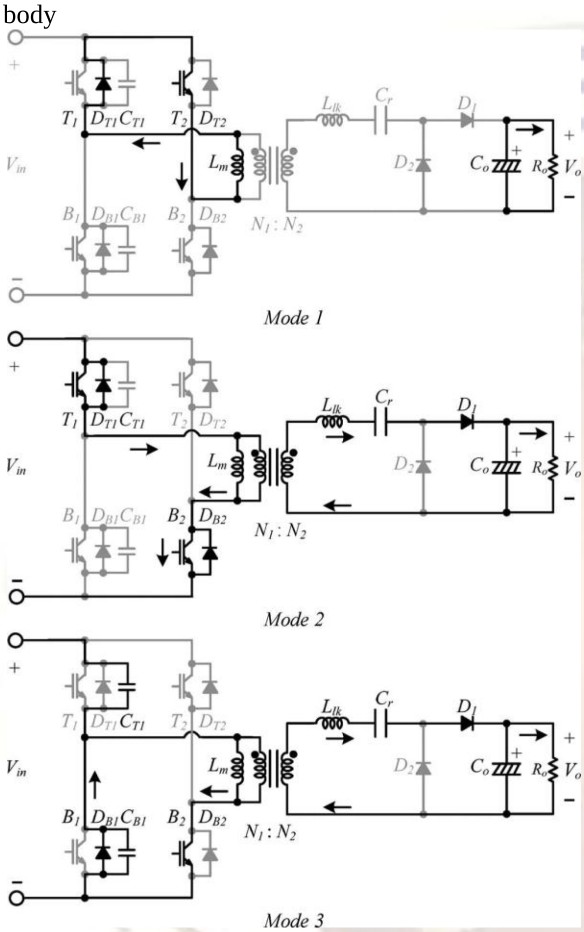

Fig3: *Modes of operation*

$$i_s(t)=i_s(t_2)\cos\omega_r(t-t_2)-\frac{V_0-v_c(t_2)}{Z_0}\sin\omega_r(t-t_2) \quad (8)$$

The following equalities are also satisfied:

$$i_p(t)=i_m(t)+ni_s(t)=-i_{B1}(t)+i_{B2}(t)$$

(9)

At the end of *Mode 3*, *is* becomes zero. Explanations of *Modes 4–6* are omitted because these modes are similar to *Modes 1–3*, respectively.

The primary current of the conventional ZVS FB converter is compared with the *ip* of the proposed converter(Fig.2).The conventional ZVS FB converter uses a large leakage inductor to achieve the ZVS of the lagging–lag switches in a wide operating range. The large leakage inductor causes higher circulating energy that significantly increases the conduction loss and further reduces the effective duty ratio. On the other hand, in the proposed converter, the effective duty ratio is not reduced, and the conduction loss from the circulating energy is relatively low by resetting the secondary current during *Mode 3* [25], [26].

To analyze the converter, two quantities are defined as frequency ratio

$$F=\frac{f_r}{f_s} \quad (10)$$

and quality factor

$$Q=\frac{4\omega_r L_{lk}}{R_0} \quad (11)$$

III. Analysis of ZVS and ZCS Conditions

In almost the entire operating range, leading-leg switches *T*1 and *B*1 are naturally turned on at zero voltage by the reflected current *is*, as shown in Fig. 2. However, to achieve ZVS and ZCS in lagging-leg switches *T*2 and *B*2, *Modes 1* and *4* have to exist, as shown in Fig. 2. In other words, the secondary current must be zero before the switching of *T*2 and *B*2. Assuming that *F* ≤ 1, there are three possible waveforms of the secondary current, as shown in Fig. 5. When the waveform of *is* is similar to Fig. 4(b), the lagging-lag switches cannot be turned off softly at zero current. On the other hand, when the waveform of *is* is similar to Fig. 4(c), *T*2 and *B*2 cannot be turned on at zero voltage. To achieve the waveform of Fig. 5(a), which is different from that of Fig. 5(b), *is* must reach zero while the secondary voltage across *N*2 is zero. Thus, *t*3, which satisfies (12), must exist

$$\begin{aligned}i_m(t_3)&=\frac{nV_{in}-(V_0-v_c(t_1))}{Z_0}\sin\omega_r(t_2-t_1)\cos\omega_r(t_3-t_2)\\&-\frac{V_0-v_c(t_2)}{Z_0}\sin\omega_r(t_3-t_2)\\&=0\end{aligned} \quad (12)$$

To achieve the waveform of Fig. 4(a), which is different from that of Fig. 4(c), the peak-to-peak value of the ripple voltage of *Cr* must be lower than *Vo*. In other words, *vc*(*t*1), which is the minimum value of *vc*, must be positive to avoid the conduction of *D*2 during *Mode 4*.

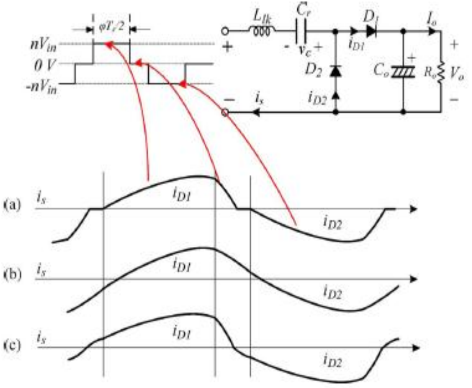

***Fig. 4:** Three possible waveforms of the secondary current is. (a) Waveform of is when IGBTs can be turned on and off softly. (b) Waveform of is when IGBTs cannot be turned off softly. (c) Waveform of is when IGBTs cannot be turned on softly.*

Therefore, from (12), thfollowing inequality must be satisfied:

$$V_0 - v_c(t_1) = \frac{V_0}{2}\left(1-\frac{\pi}{2}FQ\right) > 0 \qquad (13)$$

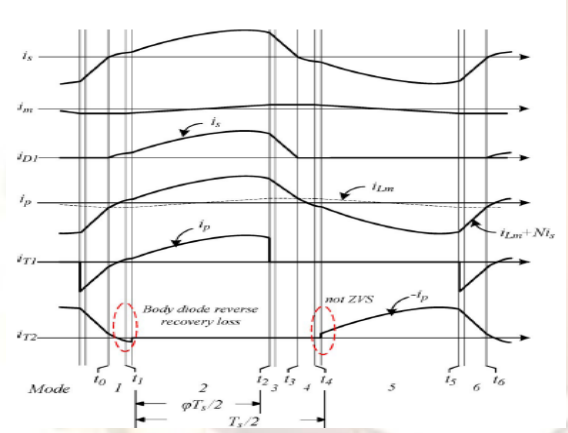

***Fig. 5:**Operation waveforms when Q is greater than 2/πF.*

Therefore, the ZVS condition of *T*2 and *B*2 is obtained as

$$Q < \frac{2}{\Pi F} \qquad (14)$$

In practical situations, *Q* may become greater than 2/*πF* under overload conditions. Fig. 7 shows the operation waveforms when *Q* > 2/*πF*. Because ZVS cannot be achieved in the lagging-leg switches, switching loss results from the body-diode reverse-recovery current and the dissipated energy of the parasitic output capacitances, as shown in Fig. 7.

However, in IGBTs, the loss resulting from non-ZVS is not large. In real switches, there are parasitic output capacitances *Coss*'s. Therefore, another ZVS condition of the lagging-leg switches is that the energy stored in *Lm* before *T*2 and *B*2 are turned on must be greater than the energy stored in the *Coss* of *T*2 and *B*2 as

$$\frac{1}{2}L_m\left(\frac{\Delta i_m}{2}\right)^2 > CossV_{in}^2$$

(15)

Where

$$\Delta i_m = \frac{\varphi v_{in}}{2L_m f_s} \qquad (16)$$

Therefore, *Lm* can be determined as

$$L_m < \frac{\varphi_{\min}^2}{32Cossf_s^2}$$

(17)

where $\phi_{\min}$ is the minimum value of ϕ satisfying the ZVS of *T*2 and *B*2. Another condition of the ZVS of the lagging-lag switches is that the dead time of the lagging leg should be short enough since the lagging-leg switches should be turned on while the current flows through the body diodes. The dead time can simply be determined by experiment.

IV. SIMULATION RESULTS

A prototype of the proposed converter was simulated through matlab. The converter was tested with *Vin* = 250 V, *Vo* = 550 V, and output power *Po* = 1.3 kW; further design parameters are given in Table I.

Fig: 6(a)&(b) shows the zero voltage and zero current i.e. soft switching waveforms of the leading leg and lagging leg switches.

TABLE 1: Simulation Parameters

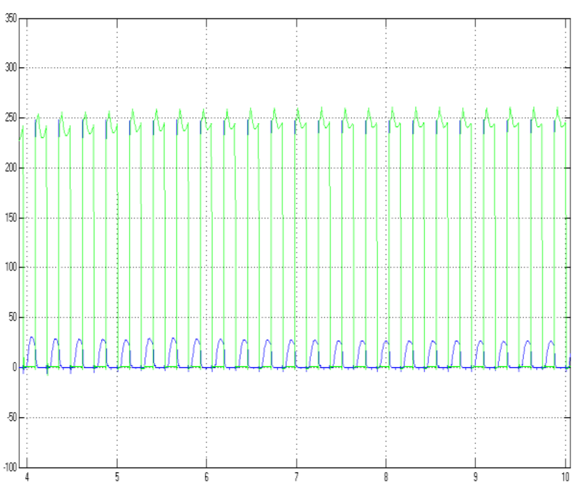

***Fig: 6(a)** soft switching waveforms of leading leg switches*

PERAMETERS	SYMBOL	VALUE
Input voltage range	V_{in}	250V
Output voltage	V_0	550V
Output power	P_0	1.3KW
Magnetizing inductance	L_m	300µH
Leakage inductance	L_{lk}	15.7µH
Quality factor at rated condition	Q	0.62
Resonant frequency	f_r	38.3kHz
Switching frequency	f_s	38.3kHz
Resonant capacitor	C_r	1.1µF
Snubber capacitor	C_{T1},C_{B1}	6.8nF

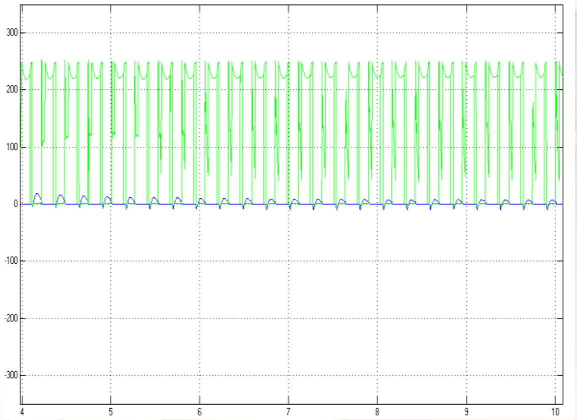

Fig: 6(b) *soft switching waveforms of lagging leg switches*

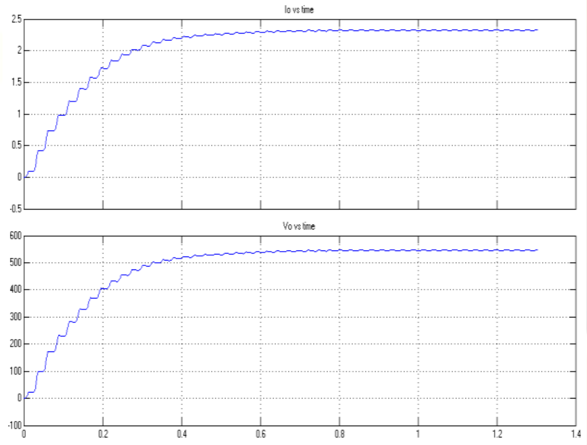

Fig7: *output voltage and current waveforms*

V . CONCLUSION

The operation of the proposed converter is analyzed. And the experimental results of a 1.2KW prototype prove the novel converter is successful. The efficiency attained under full-load conditions was over 95.5%. The converter may be adequate for high-voltage and high-power applications (> 10 kW) since the converter has many advantages, such as minimum number of devices, soft switching of the switches, no output inductor, and so on.

REFERENCES

[1] X. Wu, J. Zhang, X. Ye, and Z. Qian, "Analysis and derivations for a family ZVS converter based on a new active clamp ZVS cell," *IEEE Trans. Ind. Electron.*, vol. 55, no. 2, pp. 773–781, Feb. 2008.

[2] J. J. Lee, J. M. Kwon, E. H. Kim, and B. H. Kwon, "Dual seriesresonant active-clamp converter," *IEEE Trans. Ind. Electron.*, vol. 55, no. 2, pp. 699–710, Feb. 2008.

[3] B. R. Lin and C. H. Tseng, "Analysis of parallel-connected asymmetrical soft-switching converter," *IEEE Trans. Ind. Electron.*, vol. 54, no. 3, pp. 1642–1653, Jun. 2007.

[4] C. M. Wang, "A novel ZCS-PWM flyback converter with a simple ZCSPWM commutation cell," *IEEE Trans. Ind. Electron.*, vol. 55, no. 2, pp. 749–757, Feb. 2008.

[5] P. Das and G. Moschopoulos, "A comparative study of zero-currenttransition PWM converters," *IEEE Trans. Ind. Electron.*, vol. 54, no. 3, pp. 1319–1328, Jun. 2007.

[6] G. C. Jung, H. R. Geun, and F. C. Lee, "Zero-voltage and zero-currentswitching full-bridge PWM converter using secondary active clamp," in *Proc. IEEE PESC*, 1996, vol. 1, pp. 657–663.

[7] J. Zhang, X. Xie, X. Wu, G. Wu, and Z. Qian, "A novel zero-currenttransition full bridge DC/DC converter," *IEEE Trans. Power Electron.*, vol. 21, no. 2, pp. 354–360, Mar. 2006.

[8] T. T. Song and N. Huang, "A novel zero-voltage and zero-currentswitching full-bridge PWM converter," *IEEE Trans. Power Electron.*, vol. 20, no. 2, pp. 286–291, Mar. 2005.

[9] E. S. Kim and Y. H. Kim, "A ZVZCS PWM FB DC/DC converter using a modified energy-recovery snubber," *IEEE Trans. Ind. Electron.*, vol. 49, no. 5, pp. 1120–1127, Oct. 2002.

[10] K. W. Seok and B. H. Kwon, "An improved zero-voltage and zerocurrent-switching full-bridge PWM converter using a simple resonantcircuit," *IEEE Trans. Ind. Electron.*, vol. 48, no. 6, pp. 1205–1209, Dec. 2001.

[11] X. Wu, X. Xie, C. Zhao, Z. Qian, and R. Zhao, "Low voltage and current stress ZVZCS full bridge DC–DC converter using center tapped rectifier reset," *IEEE Trans. Ind. Electron.*, vol. 55, no. 3, pp. 1470–1477, Mar. 2008.

[12] J. Dudrik, P. Spanik, and N. D. Trip, “Zero-voltage and zero-current switching full-bridge DC–DC converter with auxiliary transformer,” *IEEE Trans. Power Electron.*, vol. 21, no. 5, pp. 1328–1335, Sep. 2006.

[13] X. Wu, X. Xie, C. Zhao, Z. Qian, and R. Zhao, “Low voltage and current stress ZVZCS full bridge DC–DC converter using center tapped rectifier reset,” *IEEE Trans. Ind. Electron.*, vol. 55, no. 3, pp. 1470–1477, Mar. 2008.

[14] R. L. Steigerwald, “A comparison of half-bridge resonant converter topologies,” *IEEE Trans. Power Electron.*, vol. 3, no. 2, pp. 174–182, Apr. 1998.

[15] R. L. Steigerwald, R.W. De Doncker, and H. Kheraluwala, “A comparison of high-power DC–DC soft-switched converter topologies,” *IEEE Trans. Ind. Electron.*, vol. 32, no. 5, pp. 1136–1145, Sep./Oct. 1996.

[16] M. Borage, S. Tiwari, and S. Kotaiah, “LCL-T resonant converter with clamp diodes: A novel constant-current power supply with inherent constant-voltage limit,” *IEEE Trans. Ind. Electron.*, vol. 54, no. 2, pp. 741–746, Apr. 2007.

[17] M. Z. Youssef and P.K. Jain, “Series–parallel resonant converter in selfsustained oscillation mode with the high-frequency transformer-leakageinductance effect: Analysis, modeling, and design,” *IEEE Trans. Ind Electron.*, vol. 54, no. 3, pp. 1329–1341, Jun. 2007.

[18] J. T. Matysik, “The current and voltage phase shift regulation in resonant converters with integration control,” *IEEE Trans. Ind. Electron.*, vol. 54, no. 2, pp. 1240–1242, Apr. 2007.

[19] S. Zheng and D. Czarkowski, “Modeling and digital control of a phasecontrolled series–parallel resonant converter,” *IEEE Trans. Ind. Electron.*,vol. 54, no. 2, pp. 707–715, Apr. 2007.

[20] R. Oruganti and F. C. Lee, “Resonant power processors. Part I—State plane analysis,” *IEEE Trans. Ind. Appl.*, vol. IA-21, no. 6, pp. 1453–1460, Nov. 1985.

[21] G. Spiazzi and L. Rossetto, “Series resonant converter with wide load range,” in *Proc. IEEE Ind. Appl. Soc. Conf.*, 1998, vol. 2, pp. 1326–1331.

[22] S. Dalapati, S. Ray, S. Chaudhuri, and C. Chakraborty, “Control of a series resonant converter by pulse density modulation,” in *Proc. IEEE INDICO*, 2004, pp. 601–604.

[23] J. G. Hayes, N. Mohan, and C. P. Henze, “Zero-voltage switching in a constant frequency digitally controller resonant DC–DC power converter,” in *Proc. IEEE APEC*, 1988, pp. 360–367.

[24] W. J. Lee, C. E. Kim, G. W. Moon, and S. K. Han, “A new phaseshifted full-bridge converter with voltage-doubler-type rectifier for highefficiency PDP sustaining power module,” *IEEE Trans. Ind. Electron.*, vol. 55, no. 6, pp. 2450–2458, Jun. 2008.

[25] B. H. Kwon, J. H. Kim, and G. Y. Jeong, “Full-bridge soft switching PWM converter with saturable inductors at the secondary side,” *Proc. Inst. Elect.Eng.—Elect. Power Appl.*, vol. 146, no. 1, pp. 117–122, Jan. 1999.

[26] J. G. Cho, J. A. Sabate, H. Guichao, and F. C. Lee, “Zero-voltage and zero-current-switching full-bridge PWM converter for high power applications,” in *Proc. IEEE PESC*, 1994, vol. 1, pp. 102–108.

[27] T. T. Song, N. Huang, and A. Ioinovici, “A zero-voltage and zero-current switching three-level DC–DC converter with reduced rectifier voltage stress and soft-switching-oriented optimized design,” *IEEE Trans. Power Electron.*, vol. 21, no. 5, pp. 1204–1212, Sep. 2006.

[28] T.-F. Chen and S. Cheng, “A novel zero-voltage zero-current switching full-bridge PWM converter using improved secondary active clamp,” in *Proc. IEEE Int. Symp. Ind. Electron.*, Jul. 9–13, 2006, vol. 3, pp. 1683–1687.

[29] E. Adib and H. Farzanehfard, “Family of zero-current transition PWM converters,” *IEEE Trans. Ind. Electron.*, vol. 55, no. 8, pp. 3055–3063, Aug. 2008.

[30] E. H. Kim and B. H. Kwon, “High step-up push-pull converter with high efficiency,” *IET Power Electron.*, vol. 2, no. 1, pp. 79–89, Jan. 2009.

[31] Y. Tsuruta, Y. Ito, and A. Kawamura, “Snubber-assisted zero-voltage and zero-current transition bilateral buck and boost chopper for EV drive application and test evaluation at 25 kW,” *IEEE Trans. Ind. Electron.*, vol. 56, no. 1, pp. 4–11, Jan. 2009.

[32] J. L. Russi, M. L. S. Martins, and H. L. Hey, “Coupled-filter-inductor soft-switching techniques: Principles and topologies,” *IEEE Trans. Ind. Electron.*, vol. 55, no. 9, pp. 3361–3373, Sep. 2009.

[33] T. Citko and S. Jalbrzykowski, “Current-fed resonant full-bridge boost DC/AC/DC converter,” *IEEE Trans. Ind. Electron.*, vol. 55, no. 3, pp. 1198–1205, Mar. 2008.

A.Suresh Kumar was born in kurnool, India. He received the B.Tech (Electrical and Electronics Engineering) degree from the Jawaharlal Nehru Technological University, Hyderabad in 2005; M.Tech (Power Electronics & Drives) from the Veluru Institute of Technology in 2008.He is currently an Asst.Professor of the Dept. of Electrical and Electronic Engineering, R.G.M College of Engineering and Technology, Nandyal. His area of interest power electronics and Electric Drives and Resonant converters.

S.Nagaraja Rao was born in kadapa, India. He received the B.Tech (Electrical and Electronics Engineering) degree from the Jawaharlal Nehru Technological University, Hyderabad in 2006; M.Tech (Power Electronics) from the same university in 2008.He is currently working as an Asst.Professor of the Dept. of Electrical and Electronic Engineering, R.G.M College of Engineering and Technology, Nandyal. His area of interest power electronics and Electric Drives..

P.BALAJI was born in kadapa,India.He received the B.Tech (Electrical and Electronics Engineering) degree from the Jawaharlal Nehru Technological University, Anantapur in 2009 . Currently perusing M-Tech (power Electronics), in Rajeev Gandhi Memorial College of Engg. & Tech,Nandyal.